NUCLEAR REACTIONS

AND

NUCLEOSYNTHESIS*

By

Richard H. Schaus

Richard J. Smith

Modified for WMU Advanced Lab Class by
Asghar Kayani, Clement Burns, and Paul Pancella

latest date: March 16, 2016

Physics Department
Montana State University
Bozeman, Montana 59717

*The development of the Nobel Lab Series was supported in part by an Instrumentation and Laboratory Improvement Grant from the National Science Foundation. (DMR-8952165)

NUCLEAR REACTIONS AND NUCLEOSYNTHESIS

I. Overview: The purpose of this laboratory is to carry out an experiment in nuclear physics where we will collide nuclei together with the help of a particle accelerator. Some of these collisions will result in new nuclei being formed, nuclei of entirely different elements. In particular, you will use a target containing lithium fluoride (LiF) and convert some of the Lithium into Helium and some of the Fluorine into Oxygen. You will detect and measure the alpha particles emitted in the processes to determine the cross section for a reaction.

Background: Transmuting one element into another was a goal of the ancient Alchemists who wanted to create gold from baser elements. Only in modern times, with the advent of experimental nuclear physics, has this actually become possible. The experiment we describe was originally created for Montana State University and has been modified for the accelerator here at WMU.

In addition to being of intrinsic scientific interest, there are many applications of nuclear physics research. Some of these applications include material analysis by nuclear backscattering, material analysis by means of nuclear reactions (charged-particle activation analysis - CPAA, prompt radiation analysis - PRA, and resonant nuclear reactions - RNR), lattice location of impurities in metals and semiconductors, and ion implantation in metals and semiconductors [Ziegler, 1975].

II. The Experiment.

1. General. We are interested in the nuclear reactions that convert lithium into helium and fluorine into oxygen. The lithium to helium reaction plays an important role in powering the sun, and understanding this reaction is necessary for understanding the physics of stars in general.

2. Experimental Overview. In this experiment we will induce certain low-energy, light-particle nuclear reactions in which selected target materials are bombarded by protons or alpha particles accelerated in the Van de Graaff linear accelerator to energies of 0.5 to 2.0 MeV. The results will be analyzed by alpha particle spectroscopy as appropriate to confirm the reaction. For the sake of clarity in the following sections we only discuss charged particle spectroscopy. Detection of neutral particles requires different techniques.

3. Laboratory Apparatus. The following is a brief description of the major laboratory apparatus which we will use in this experiment.

a. The Particle Accelerator. A Tandem Van de Graaff linear accelerator capable of producing a beam current of up to several microamperes of collimated protons or alpha particles (and other heavier ions), with incident energies at the target of 0.5 to 12 MeV (multi- charged ions can be accelerated to even higher energies) will be used. While the electrical beam current is most easily measured, it will also be useful to think of the accelerated particle beam in terms of the number of ions delivered at the target in a given interval of time. For example, a beam current of 1 μA means that a total electric charge is delivered to the target at a rate of10^{-6} C/s . In terms of numbers of protons (^{1}H) or singly-ionized alpha particles (^{4}He), this equates to about 6.24 x 10^{12} particles/s incident at the target, simply using the known electric charge of each beam particle.

To produce an accelerated beam of positive ions requires an ion source, an accelerating voltage, an evacuated acceleration path with associated vacuum system, and a control system. The Tandem Van de Graaff accelerator that we will use has two *negative* ion sources, called respectively SNICS and Duoplasmatron, which can essentially be interchanged, depending on the type of beam particle desired. The negative ions are then electrically injected into the acceleration path where they are accelerated by the high-voltage gradient along the accelerator column. At the center of the tandem tank, the electrons are stripped from these ions just as they pass the point of greatest positive voltage relative to ground. Thus the ions become positively charged and get another stage of acceleration as they leave the positively charged terminal, ultimately returning to ground potential.

The high-voltage for the acceleration path is produced and maintained on the generator's hemispherical terminal shell by means of beaded chains, called a pelletron system, which conveys charges between ground potential and the shell (removing electrons from the shell). The shell, the voltage insulating column which supports the shell and the chain charging system which maintain the column's voltage gradient, including the charging chain drive motors, are all enclosed in a dry-inert-gas-filled pressure vessel to provide for electrical isolation of the high voltage from ground potential. The pelletron charging current is controlled by an adjustable dc source on the operation console in the laboratory control room.

b. Particle Detectors. Charged particle spectroscopy is the form of reaction analysis we will use when a product of a given nuclear reaction is an alpha particle or other charged particle. The detector is a relatively simple semiconductor diode (surface barrier) device. Target and detector are both mounted in a vacuum chamber, which is equipped with feedthroughs which allow them to be moved from outside. The sensitive face of the detector views the target head on, i.e., it is normal to a line joining its center with the center of the target. (Target center is defined as the point where the well-collimated beam intersects the target.) This line and the beam are in the same horizontal plane, which thus includes the centers of both target and detector. The scattering angle θ viewed by the detector can be adjusted from 0° to about 170° relative to the particle beam path. Note that all angles in this writeup are specified in the laboratory frame of reference. Thus $\theta = 180°$ would represent a backscattered trajectory.

The detector's active surface area is about 50 mm^2, although in some experiments you may define a smaller active area with a physical aperture located directly in front of the detector. The detector is typically mounted a few cm from the target, such that the solid angle, Ω, subtended by the particle detector is about 0.02 steradian. You may determine the actual solid angle for your own measurements, or this factor will be given to you.

Since the essence of the performance of this experiment lies in the detection and qualitative and quantitative analysis of the energetic particle products of the reaction to confirm the actual nuclear reaction, it is desirable to fully understand the principles of operation of the detectors.

Semiconductor charged particle detectors have been used extensively in experimental nuclear research since the mid-1960's, and are now used nearly exclusively for such. They can be used over a very wide range of energies, from 20 keV electrons through 200 MeV heavy ions for example, with good inherent resolution. Additionally, semiconductor gamma and x-ray detectors are contributing significantly in the field of photon spectroscopy.

A semiconductor diode detector is essentially a reverse-biased p-n junction with a depletion region at the p-n interface which prohibits current flow. The thickness of the first doped layer and the applied bias combine to produce the smallest possible dead layer at the entrance to the active detector volume. When an energetic particle passes through the depletion region, electrons are

excited into the conduction band and holes are formed in the valence band. The electrons are swept toward the positive (n) side of the junction, and the holes toward the negative (p) side by the internal electric field which is enhanced by the bias voltage. A brief current pulse is thus created by the passage of the otherwise invisible particle, which can be measured with the appropriate electronics.

The two principle quantities of interest measured by the detector are:

(1) Particle Energy The magnitude of the current pulse is proportional to the number of electrons excited into the conduction band (3.6 eV/excitation), and hence to the number of interactions undergone by the incoming particle before giving up its kinetic energy. We assume that the depletion region of the detector is sufficiently thick (typically 100 μm in our lab) to completely stop the charged particle, i.e. all of the kinetic energy of the particle will be used up in making electron-hole pairs.

(2) Rate (#/sec) of particle emission This is proportional to the frequency of arrival of the current pulses in the detector.

c. Amplifiers It is normally necessary to have at least two stages of amplification to allow for accurate measurements of the very small current pulses from these surface barrier detectors. The first stage, called a preamplifier, or "pre-amp", is located very near the detector itself to minimize signal degradation in cables. By placing the current pulse across a very high impedance, the signal is converted to a voltage pulse for transmission out of the target area and into the counting area. The pre-amp will normally have a fixed gain, and a "test" port. Artificial current pulses from a device called a "pulser" may be fed to the test port in order to aid in calibration. The detector bias voltage is also supplied through the pre-amp module.

Another amplifier with adjustable gain receives the pulses from the pre-amp. The gain of this amplifier is adjusted to place the events of interest into an appropriate part of the MCA spectrum (see below). In many cases (including ours) this means amplifying to the point where pulse heights are in the range of a few volts.

There are many details of these amplifiers that we can gloss over for our present purposes. Their most important feature for us is that they respond linearly over a wide range of pulse heights. We will effectively test this feature for the whole chain of data processing when we calibrate our detector system.

d. The Multichannel Analyzer Following the chain of amplifiers, the multichannel analyzer (MCA) is a special-purpose computer which provides for acquisition, storage, display, and analysis/interpretation of the data from our detector. In our case, the multichannel analyzer consists of a plug-in card in a desktop computer, and is sometimes referred to as a PCA (personal computer analyzer). The MCA/PCA can be used in either of two data analysis modes - the pulse height analysis (PHA) mode, or the multi-channel scaling (MCS) mode. The PHA mode is used nearly exclusively for backscattering spectrometry, and is the mode we will use for this experiment. The MCS mode is used in applications where the numbers of particles detected (counts) are needed as a function of time, regardless of the particle energy.

In the PHA mode, a spectrum (histogram) of the frequency distribution of pulse heights (particle energies) is accumulated from the input pulses received from the detector through the preamp/amplifier system. The different pulse heights of the pulses are assigned to channel numbers which are proportional to pulse height (energy), and simultaneously displayed in real time and stored in memory for subsequent analysis.

4. Nuclear Reaction Analysis Techniques. We may classify any given interaction as either a nuclear or non-nuclear reaction through an analysis of the energies involved. Recall that both the target nucleus and the beam particle are positively charged. The strong nuclear force has a very short range, measured in Fermis (10^{-15} m). Only if the beam particle has sufficient kinetic energy will it get close enough to the target nucleus for the strong force to have any effect. Up to that point, the electrostatic (Coulomb) force dominates and determines all trajectories.

Let's call that critical distance between the projectile (beam particle) and target nucleus R, the separation at which the strong nuclear attractive force just equals the electrostatic (Coulomb) repulsive force, F. Then the amount of work done by an external force to move the two particles from infinite separation to a distance R apart is given by:

$$W = \text{PE} = \int_{\infty}^{R} F\, dr$$

This amount of work done against the Coulomb repulsive force represents the height of the potential barrier (PE) which must be exceeded in order that a nuclear reaction might occur. If KE represents the total kinetic energy available in the initial state (due to the beam) then:

if KE/PE is
- >1 : Nuclear Reaction may occur
- <1 : Non-Nuclear Rutherford Scattering will usually occur

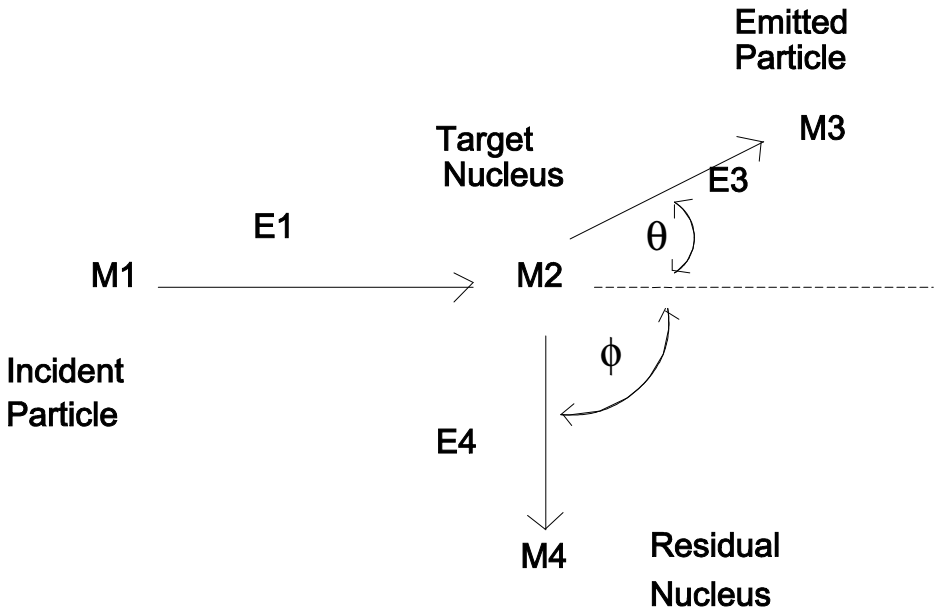

Figure 1. Schematic Diagram and definition of kinematic variables.

where:
- M1,E1 = mass and energy of the incident (beam) particle
- M2,E2 = mass and energy of target nucleus
- M3,E3 = mass and energy of emitted (detected) particle
- M4,E4 = mass and energy of residual nucleus (undetected)
- θ = scattering angle of the emitted (detected) particle
- ϕ = scattering angle of residual nucleus, both angles in lab frame

A symbolic continuity equation for the general interaction diagrammed in Fig. 1 is:

$$M1 + M2 \Rightarrow M3 + M4 + Q$$

or in standard nuclear reaction notation:

$$M2(M1,M3)M4$$

where Q may be defined as the energy released or absorbed in the reaction, or the difference between the total rest energy of the system before and after the reaction. Since the binding energies of nuclei are significant compared to their rest energies, we must make use of the relativistic equivalence between mass and energy. Specifically:

$$Q = \delta(mc^2) = (M1 + M2)c^2 - (M3 + M4)c^2$$

where: $Q>0$ => exoergic reaction
$Q<0$ => endoergic reaction

In all, there are four basic types of interactions which we may encounter at the energies reachable by our accelerator, three of which involve nuclear reactions. The other is Rutherford scattering, completely determined by the Coulomb force. Although our interest in this experiment is in nuclear reactions, all four types of interactions may influence our experiment, and we will have to account for all of them in our detection plan.

The nuclear reactions may be categorized according to three basic mechanisms: (1) direct capture of the incident particle by the target nucleus to form a compound nucleus which then decays by the emission of gamma ray(s) (M3=0 because particle 3 is a photon, E3 is the photon energy); (2) inelastic scattering of the incident particle, in which part of the incident energy is absorbed by the target nucleus, which is then left in an excited state (M1=M3, M2=M4, E3≠E1, Q≠0); and (3) rearrangement collisions in which the particles which separate after a collision are different from those which entered into the collision (M1≠M3, E3≠E1, Q≠0).

These basic reaction mechanisms provide different reaction scenarios on which we will need to base our detection plan. Analysis of radioactivity produced in a nuclear reaction and detected afterward, as in measurement of the radiation emitted from a radioactive product nuclide, is termed activation analysis. Detecting and measuring the reaction yield of energetic particles such as alpha particles and gamma rays at the instant of reaction is termed prompt radiation analysis (PRA). In this experiment we shall perform prompt radiation analysis of nuclear reactions of types proton-alpha (p,α).

Figure 2. Energy Analysis of a Nuclear Interaction.

.... KE/PE > 1 > KE/PE.....

. .

. .

Nuclear Reactions

Direct Capture
M3=0
E3=γ
Q≠0

Inelastic Scattering
M3=M1
M4=M2
E3≠E1
Q≠0

Rearrangement Collisions
M3≠M1
M4≠M2
E3≠E1
Q≠0

Non-Nuclear Interaction

Rutherford (elastic)Scattering
M3=M1
M4=M2
Q=0

where: γ = photon

$$W = \text{PE} = \int_{\infty}^{R} F\, dr$$

F = Electrostatic (Coulomb) Force $F = k(q_1)(q_2)/r^2$
q_1, q_2 = point charges of beam particle and interacting nucleus
k = Coulomb's constant
r = charge separation distance
R = inter-nuclear distance at which the Strong Nuclear Force equals the Coulomb Force for a given pair of particles

Reaction Yield and Differential Cross Section.

(1) Reaction Yield $Y(\theta)$: A fundamental part of a laboratory nuclear reaction experiment is *measuring* the reaction yield, Y, as a function of detection angle θ, where $Y(\theta)$ is expressed as the number of reactions produced and observed at detection angle θ [Ziegler, 1975].

[1] $Y(\theta) = \sigma(\theta,E)\, n\, N\, \delta x\, \Omega$

where:

n = number of incident beam particles
N = number of target atoms/cm^3
δx = target thickness in cm probed by the beam
Ω = detector solid angle
$\sigma(\Theta,E)$ = differential cross section (cm^2/steradian)

and where:

$N = \rho N_o/M$
ρ = mass density of target (gm/cm^3)
N_o = Avogadro's Number (atoms/mole)
M = atomic mass of target (gm/mole)

(2) Reaction Differential Cross Section $\sigma(\theta,E)$: The reaction differential cross section, which is a function of detection angle θ and incident particle energy E, is *calculated* using the measured yield. This cross section is expressed in units of cm^2/steradian, and is defined as [Ziegler, 1975]:

[2] $\sigma(\theta,E) = Y(\theta)/(n\, N\, \delta x\, \Omega)$

5. Setting Up The Experiment.

a. General. Preparing a nuclear reaction experiment involves a logical sequence of decisions and calculations prior to the actual conduct of the experiment. In general this sequence involves the following steps.

(1) Decide upon a particular reaction which is appropriate to both the experimental objective(s) and the particular laboratory capabilities and constraints.

(2) Calculate the Q-value of the planned nuclear reaction (Figure 4):
[3] $Q = (M1 + M2)c^2 - (M3 + M4)c^2$.

(3) When the emitted reaction product of interest is an alpha particle, the next step in the sequence will be to decide upon an appropriate incident particle energy, E1, and detection angle, θ, to use for the experiment. The parameters involved in choosing E1 and θ for the alpha product include: the particular reaction requirements, experimental objective(s), and

accelerator capabilities. Another principle factor involved in choosing E1 and θ will be whether the energy differential between the emitted alpha particles and the non-reacting, Rutherford-scattered incident particles is sufficiently great so that the reaction products are sitting on a zero background. Thus, while the values for E1 and θ initially chosen may prove to be appropriate, it may be that other values must be tried in order to provide a sufficient energy "separation" of the product particles.

Steps (1) and (3) involve subjective decisions based upon particular experimental objectives and constraints, and laboratory capabilities. Step (2) involves calculations discussed under Nuclear Reaction Analysis Techniques.

b. Energy of the Emitted Particle . One of the first steps in setting up a nuclear reaction experiment, after deciding upon the reaction to be performed, is to calculate the theoretical energy of the emitted particle in the direction θ relative to the direction of travel of the incident particle in the laboratory given the type of incident particle, its planned energy, and the nature of the target material. This is done by the conservation of total energy and momentum in the non-relativistic case.

Referring to Figure 4, we have that [Feldman, 1986]:

[4] $$E3^{1/2} = A \pm (A^2 + B)^{1/2}$$

where:

$$A = [(M1 \times M3 \times E1)^{1/2}/(M3 + M4)] \cos(\theta)$$

$$B = [M4 \times Q + E1(M4 - M1)]/(M3 + M4)$$

which shows that E3 characterizes a given reaction for specific values of E1 and θ, such that the energy spectrum E3 will be a function of the Q values possible in the reaction. Furthermore, analogous to optical spectroscopy, if the residual nucleus can be left in any of several sharply defined energy states, and if the target is thin so that the incident energy has a single, well-defined value, the energy spectrum of the emitted particles will exhibit a series of narrow peaks, each of which corresponds to one of the excited states of the residual nucleus. This spectrum will then be specific to the reaction and can be used to identify the presence of a given elemental isotope. This same equation, but in a different form, is given by Ziegler (1975) in Chapter 3, p.188.

6. Safety. In addition to normal electrical and mechanical safety hazards typical of electromechanical instrumentation, a potential hazard in working with positive ion accelerators is *Bremsstrahlung* radiation induced by high energy electrons, and neutrons from (p,n) and (α,n) nuclear reactions.

High x-ray fluxes may be produced by electrons, created by beam ionization of background gas, being accelerated into the high-voltage terminal shell. By maintaining an appropriate pumping speed in the beam line system, the amount of residual gas in the accelerator tube and scattering of the ion beam as it leaves the ion source can be reduced, thus greatly reducing the potential for *Bremsstrahlung* radiation.

The other main hazard is neutrons from nuclear reactions between the accelerated ion and the target material. However, since one of our experimental boundary conditions is that no reactions involving neutrons will be performed, then strict adherence to well-documented incident particle energy levels and knowledge of possible neutron-producing reactions will avoid neutron production and associated radiation hazards. Chu *et al* (1978) in Table 6.1 provide data of interest regarding some troublesome neutron-producing reactions. In particular, note that the threshold for neutron production in the $^{7}Li(p,n)^{7}Be$ is at 1.88 MeV. **Do not run the accelerator above 1.8 MeV when working with the LiF sample.**

7. A Menu of Nuclear Reactions. Figure 6 is a list of nuclear reactions of potential interest that we could carry out, divided into categories of Calibration, Stellar Nucleosynthesis, and General Interest reactions. Note that we will not be carrying out all these reactions. The reactions we will carry out are listed in bold.

Figure 3. Menu of some Nuclear Reactions.

Reactions Relevant for Stellar Nucleosynthesis

$^{7}Li(p,\alpha)^{4}He$	**1500**	**C, F&M, M&R p 118**
$^{12}C(p,\gamma)^{13}N$	1698	M&R p216, Z p 182
$^{15}N(p,\alpha)^{12}C$	800	C, F&M, M&R p 118
$^{16}O(p,\gamma)^{17}F$	1514	Z pp 179-182

General Interest

$^{19}F(p,\alpha)^{16}O$	**1250**	**C, F&M, M&R p 119**
$^{19}F(p,\alpha\,\gamma)^{16}O$	874	M&R p 167

Reference Key

C - Chu *et al*, (1978), Table 7.8, p 213
F&M - Feldman and Mayer, (1986), Table 12.2, p 307
M&R - Mayer & Rimini, (1977)
Z - Ziegler, (1975)

8**. Schedule for Experiment and Report.** The following is the suggested procedure for this experiment and writeup:

Begin reading about the experiment as discussed here to get familiar with the experimental, the references, and the laboratory equipment and instrumentation.

Before coming to lab work the following problems, and be prepared to hand in all calculations and comparisons at the beginning of lab. See the discussion in Section III.5 and in Appendix A for guidance in working these problems.

(1) Consider the reaction $^{7}Li(p,\alpha)^{4}He$, and the following reaction values :

Projectile Ion Energy, E1 = 2.0 MeV
Alpha Lab Detection Angle = 150^{0}
Target Thickness = 100 nm
Reactions Counted = 1000
Integrated Accelerator Beam Charge = 2.0×10^{-4} C
Alpha Detector Solid Angle = 0.002 steradian
Note: these values *may* be different from those you will actually encounter in the lab, and are intended only for the homework problem.

Using the analytical expressions discussed herein, calculate manually, the following quantities:

Reaction Energy, Q, in MeV
Emitted Particle Energy, E3, in MeV
Kinematic Factor, K
Maximum Energy of Rutherford-Scattered Particle in MeV
Differential Cross Section in millibarns/steradian
Yield in # of reactions/μC

In the lab, Day 1:
Our first day will be used to introduce the accelerator and the required detector and data acquisition systems. After setting up the chamber with a detector and a variety of selectable targets, we will run proton beam at a fixed energy to illustrate the operation of the PCA/MCA system.

Our most relevant data will be the energies of detected alpha particles resulting from various nuclear interactions. It is crucial that these energies be measured as accurately as possible, with good resolution. Therefore, most of our first day in the lab will be spent acquiring data for energy calibration, and understanding how to use that data.

Energy calibration simply means knowing exactly what detected particle energy corresponds to each channel (or bin) in the MCA spectrum (histogram). Since this is so important, we will actually take two different sets of data to help us determine this.

The entire system may be calibrated if particles with at least three different known energies can be provided to the detector. We will do this using Rutherford Backscattering (RBS) from three or four different elements. If the mass of the struck nucleus is known, along with the beam particle mass and energy, and scattering angle, then the maximum energy of the scattered beam particle is

completely determined. We will illustrate how this maximum energy appears on a sample RBS spectrum, then collect data on additional targets for later analysis.

We expect that our detector-amplifer-MCA system behaves linearly across the range of energies we are interested in detecting. To help confirm this expectation, we will also take data with a "pulser" module. This module simply generates artificial current pulses which are fed to a special input on the preamp. The amplitude of these pulses can be controlled precisely, so that the ratio between different test pulses can be known accurately. You will choose enough ratios to check the linearity of your detector system, as well as verifying the magnitude of any zero offset.

In the lab, Day 2: As directed by your instructor, set up an experiment to measure the following two reactions

$$^{7}Li(p,\alpha)^{4}He \quad \text{and } ^{19}F(p,\alpha)^{16}O$$

You will use a metal sample with a thin film of LiF evaporated onto the surface. The thickness of the LiF is 200±20 Å. You may or may not have to make additional measurements to determine the solid angle of the detector.

Points which you should consider in your analysis include: 1) a comparison of the measured and calculated energies of the α peaks from the reactions; 2) the yield obtained from each reaction and how it compares to the expected yield using tabulated cross sections; 3) the width of the two α peaks, and 4) the various contributions to the widths of the peaks, such as sample thickness, uniformity of the sample and foil thickness, etc. 5) compute the relative cross sections (that is, the ratio of the cross sections) for Li and F reactions as a function of energy. **Be sure to estimate the errors in all of the quantities you measure!**

IV. Suggested Readings.

1. For Historical/Research Background on Stellar Nucleosynthesis.

a. "Experimental and theoretical nuclear astrophysics: the quest for the origin of the elements", Fowler (1984).

b. Nuclear Astrophysics, Fowler (1967).

c. "Two decades of collaboration with Willy Fowler", by Fred Hoyle, Barnes *et al* (1982).

2. For Theoretical/Computational Background.

a. Chapters 2, 3, and 12, Fundamentals of Surface and Thin Film Spectroscopy, Feldman and Mayer (1986).

b. Chapters 1, 2 and 4, Ion Beam Handbook for Material Analysis, Mayer and Rimini (1977).

V. References.

Ashcroft, N.W., and Mermin, N.D., 1976, Solid State Physics, Saunders College, Philadelphia.
Barnes, C.A., Clayton,D.D., and Schramm, D.N., 1982, Essays in Nuclear Astrophysics, Cambridge University Press, Cambridge.
Burbidge, E.M., Burbidge, G.R., Fowler, W.A., and Hoyle, F., 1957, Reviews of Modern Physics, 29:4, 547.
Chandrasekhar, S., 1984, Reviews of Modern Physics, 56:2/1, 137.
Chu, W.K., Mayer, J.W., and Nicolet, M.A., 1978, Backscattering Spectrometry, Academic Press, New York.
Feldman, L.C., and Mayer, J.W., 1986, Fundamentals of Surface and Thin Film Spectroscopy, North Holland, New York.
Fowler, W.A., 1967, Nuclear Astrophysics, American Philosophical Society, Philadelphia.
Fowler, W.A., 1984, Reviews of Modern Physics, 56:2/1, 149.
Mayer, J.W., and Rimini, E.(eds), 1977, Ion Beam Handbook for Material Analysis, Academic Press, New York.
Northcliffe, L.C., and Schilling, R.F., 1970, Nuclear Data Tables, A7, 233.
Ortec, 1976, Applications Note 34, Experiments in Nuclear Science, 2nd Ed, Ortec Inc, Oak Ridge, TN.
Physics Today, 1984, 37:1, 17.
Ziegler, J.F.(ed), 1975, New Uses of Ion Accelerators, Plenum Press, New York.

Appendix A: Computational Summary, additional tools

1. Reaction Energy: Equation [3] and Figure 4:

$$Q = (M1 + M2)c^2 - (M3 + M4)c^2$$

2. Emitted Particle Energy: Equation [4] and Figure 4:

$$E3^{1/2} = A \pm (A^2 + B)^{1/2}$$

$$A = [(M1 \times M3 \times E1)^{1/2}/(M3 + M4)] \cos \theta$$

$$B = [M4 \times Q + E1(M4 - M1)]/(M3 + M4)$$

3. Kinematic Factor: Equation [5] and Figure 4:

$$K = \{[M1 \cos \theta + (M2^2 - M1^2 \sin^2 \theta)^{1/2}]/(M1+M2)\}^2$$

4. Rutherford-Scattered Particle Energy: Equation [6] and Figure 4:

$$KE1 = K \times E1$$

5. Yield: Equation [1]:

$$Y(\theta) = \sigma(\theta,E)\, n\, N\, \delta x\, \Omega$$

Note a: Referring to Chapter 4 of Ashcroft and Mermin (1976):

$$N \text{ for Al} = 4 \text{ atoms}/(4.05 \text{ E-08 cm})^3 = 6.02 \text{ E22 atoms/cm}^3$$

$$N \text{ for Li} = N \text{ for F} = 4 \text{ atoms}/(4.02 \text{ E-08 cm})^3 = 6.16 \text{ E22 atoms/cm}^3$$

$$N \text{ for LiF} = 4 \text{ molecules}/(4.02 \text{ E-08 cm})^3 = 6.16 \text{ E22 molecules/cm}^3$$

Note b: In calculating the Yield, Y, for a given reaction in which the thickness of the target material is unknown, it is convenient to calculate the ratios of the yields of alpha peaks for the different incident proton energies used. If a constant integrated beam charge is used for all incident proton energies, the values of the variables n, N, δx, and Ω all remain constant throughout a given reaction. The resulting ratios of the differential cross sections as functions of incident proton energy may then be compared to the ratios of established (published) cross sections for like reactions and incident proton energies as an initial check on your results.

6. Differential Cross Section: Equation [2]:

$$\sigma(\theta,E) = Y(\theta)/(n\ N\ \delta\ x\ \Omega)$$

7. Range of Rutherford-scattered particles in aluminum foil:

Refer to Nuclear Data Tables of Northcliffe and Schilling (1970). As an example for a 0.4031 MeV proton in aluminum, enter the ^{1}H Ion Range Table on p 255 with 0.4031 MeV in the right-hand column; under the column headed Al read a range of 1.179 mg/cm^2. To convert this to microns of aluminum, use the conversion formulae on p 253. In this case, multiplying the tabular range of 1.179 by ten divided by the density of aluminum (10/2.6989) results in a range of 4.37 μm in aluminum. Thus, in order to stop this particular Rutherford-scattered proton from entering the detector, we would need to use an aluminum absorber foil at least 4.37 μm thick. The range obtained from the polynomial fit in section III.5 of this manual is 4.41 μm, in good agreement with the tabulated value.

8. Energy loss of emitted alpha particles in passing through the aluminum absorber foil:

Refer to the Nuclear Data Tables of Northcliffe and Schilling (1970). As an example for a 5.0033 MeV alpha particle passing through 10 μm of aluminum absorber foil, enter the ^{4}He Ion Electronic Stopping Power Table on p 256 with 5.0033 MeV in the right-hand column; under the column headed Al read an electronic stopping power of 0.598 MeV/mg/cm^2. To convert this to MeV/μm of aluminum, use the conversion formulae on p 253. In this case, multiplying the tabular stopping power of 0.598 by the density of aluminum divided by 10 (2.6989/10) results in a stopping power of 0.161 MeV/μm of aluminum. Multiplying this by the foil thickness of 10 μm results in a loss of 1.61 MeV by the emitted alpha particle in passing through the absorber foil. Thus, we could expect to <u>detect</u> the alpha particles at an energy of 5.0033 MeV - 1.61 MeV ≅ 3.39 MeV. The stopping power obtained from our polynomial fit in section III.5 is also 1.61 MeV. Note that assuming a constant stopping power throughout the foil may not be a good approximation for thicker foils. You can improve your calculation by using an average stopping power based on the average energy of the particle traveling through the foil. You could also step your way through the foil in an iterative calculation using thickness increments for which a constant stopping-power value is a good approximation.

9. Estimated target thin film thickness using experimentally determined reaction yield together with published differential cross section as a function of incident energy data for a particular reaction:

Use Equations [1] or [2] in the form:

$$\delta x = Y(\theta)/(n\ N\ \Omega\ \sigma)$$

Energy Straggling and Peak Widths

The widths of the peaks in the energy distribution curve are determined primarily by two factors, detector resolution and energy straggling. Energy straggling is the term used to describe the *spreading* in the energy distribution which occurs as the ions pass through the material. Because the individual ion trajectories and encounters will vary from one ion to the next, the ions which emerge from a thin foil (thickness δx) will have a greater spread in energy than they did upon entering the foil. Thus the peak width of the particles upon entering the foil may be very narrow (like that from the ^{210}Po source), while the emerging ions will have a shifted, broader energy distribution. The energy shift is associated with the energy loss process (stopping power), while the broadening is associated with energy straggling. If the two broadening mechanisms (detector resolution and straggling) are independent of one another, their combined effect can be estimated by adding the squares of the individual contributions

[9] $$W^2 = W_R^2 + W_x^2 + W_{ST}^2 + W_{SF}^2$$

where:

W = Full-Width-at-Half-Maximum (FWHM) of the alpha peak in the measured energy distribution spectrum (keV);

W_R = FWHM broadening associated with the detector resolution, ≈ 20 keV

W_{ST}^2 = FWHM broadening (squared) due to Bohr energy straggling in LiF (statistical fluctuations in the energy loss of the emitted alpha particle exiting target material). [Section 1.4 and Table 1.2, Mayer and Rimini, 1977; Chapter 4, Ashcroft and Mermin, 1976].

$$\approx [0.79\text{E-}02\ \text{keV}^2/\text{A}]\ \delta x / \left|\text{Cos}\ \theta_{lab}\right|$$ for the case of LiF produced α's (α energies about 7 MeV)

W_{SF}^2 = FWHM broadening (squared) due to energy straggling in the <u>aluminum stopper foil</u>. Here, t_f is the thickness of the stopper foil.

$$\approx t_f\ [0.82\text{E-}02\ \text{keV}^2/\text{A}]$$

W_x = FWHM broadening associated with the energy loss (stopping power) of the α particles for a sample of finite thickness (δx). That is, reactions occur throughout the film thickness and reaction products lose an amount of energy depending on the depth at which the reaction occurs. The stopping powers for α particles in LiF are tabulated [Section 1.4 and Table 1.1, Mayer and Rimini, 1977; Nuclear Data Tables, pp 253-257, Northcliffe and Schilling, 1970]. For the Li and F reactions studied here

$$\approx [1.46\text{E-}02\ \text{keV/A}]\ \delta x / \left|\text{Cos}\ \theta_{lab}\right|$$

We neglect energy losses and straggling associated with the incident proton beam as it passes through the target material (Why?).

Film thickness using Rutherford Backscattering Spectrometry (RBS)

Refer to Sections 2.3 and 3.5, and to Equation (3.20b) on p 49 of Feldman and Mayer (1986), which relate the "energy width" of the backscattering spectrum to the thickness of the target film. Use a beam of alpha particles for this measurement, and use the width of the scattered alpha peak from ^{19}F in this procedure rather than the ^{7}Li alpha peak (Why?). If the film thickness δx _ 1000 A, the "surface energy approximation" may be used, in which case, from Equation (3.20b), $[dE/dx]_{in}$ is evaluated at the incident alpha particle energy, E1, and $[dE/dx]_{out}$ is evaluated at the energy of the Rutherford-scattered alpha particle, KE1. The electronic stopping power tables for ^{4}He ions given by Mayer and Rimini (1977), Feldman and Mayer (1986), or Chu *et al* (1978) may be used for values of [dE/dx]. However, since the target material, LiF, is a compound, its electronic stopping power for ^{4}He ions must be calculated using the electronic stopping powers of Li and F in accord with the Bragg additivity rule. For LiF this electronic stopping power becomes

$$[dE/dx]_{LiF} = N \{ \varepsilon_{Li} + \varepsilon_{F} \}$$

where ε_i is the stopping cross section for element i as found in the tables mentioned above, and N is the number density for LiF, #molecules/cm^3. Using the surface energy approximation, the film thickness then becomes

$$\delta x = \delta E1 \{[K [dE/dx]_{E1} + | \text{Cos } \theta_{lab} |^{-1} [dE/dx]_{KE1}\}^{-1}$$

where $\delta E1$ is the Full Width at Half Maximum (FWHM) of the Rutherford-scattered alpha peak resulting from a film of thickness δx. **Caution**: Ensure that you are consistent in your use of units of thickness when dealing with the film and with the electronic stopping power.